ARTICLE

Oligosaccharyltransferase-Subunit Mutations in Nonsyndromic Mental Retardation

Florence Molinari,[1] François Foulquier,[2,3] Patrick S. Tarpey,[4] Willy Morelle,[3] Sarah Boissel,[1] Jon Teague,[4] Sarah Edkins,[4] P. Andrew Futreal,[4] Michael R. Stratton,[4] Gillian Turner,[5] Gert Matthijs,[2] Jozef Gecz,[6,7] Arnold Munnich,[1] and Laurence Colleaux[1,*]

Mental retardation (MR) is the most frequent handicap among children and young adults. Although a large proportion of X-linked MR genes have been identified, only four genes responsible for autosomal-recessive nonsyndromic MR (AR-NSMR) have been described so far. Here, we report on two genes involved in autosomal-recessive and X-linked NSMR. First, autozygosity mapping in two sibs born to first-cousin French parents led to the identification of a region on 8p22-p23.1. This interval encompasses the gene *N33/TUSC3* encoding one subunit of the oligosaccharyltransferase (OTase) complex, which catalyzes the transfer of an oligosaccharide chain on nascent proteins, the key step of N-glycosylation. Sequencing *N33/TUSC3* identified a 1 bp insertion, c.787_788insC, resulting in a premature stop codon, p.N263fsX300, and leading to mRNA decay. Surprisingly, glycosylation analyses of patient fibroblasts showed normal N-glycan synthesis and transfer, suggesting that normal N-glycosylation observed in patient fibroblasts may be due to functional compensation. Subsequently, screening of the X-linked *N33/TUSC3* paralog, the *IAP* gene, identified a missense mutation (c.932T→G, p.V311G) in a family with X-linked NSMR. Recent studies of fucosylation and polysialic-acid modification of neuronal cell-adhesion glycoproteins have shown the critical role of glycosylation in synaptic plasticity. However, our data provide the first demonstration that a defect in N-glycosylation can result in NSMR. Together, our results demonstrate that fine regulation of OTase activity is essential for normal cognitive-function development, providing therefore further insights to understand the pathophysiological bases of MR.

Introduction

Mental retardation (MR), defined as an intelligence quotient below 70, is the most frequent handicap in children, affecting 1% to 3% of the general population.[1] Despite recent advances, the causes of nearly 40% of MR remain unclear. Although a considerable number of X-linked MR (XLMR) genes are known, only four genes causing autosomal-recessive nonsyndromic MR (AR-NSMR) have been identified so far: *PRSS12* (MIM 606709),[2] *CRBN* (MIM 609262),[3] *CC2D1A* (MIM 610055),[4] and *GRIK2* (MIM 138244).[5] These genes are involved in different pathways, namely synaptic proteolysis, regulation of mitochondrial energy metabolism, regulation of I-κB kinase/NF-κB cascade, and induction of long-term potentiation (LTP), underlining the extreme heterogeneity of the pathophysiological mechanism involved in these diseases.

Glycosylation is an important posttranslational modification that occurs in every cell and has a significant impact on numerous biological processes. Many defects in the asparagine-linked glycosylation (N-glycosylation) have been identified in congenital disorders of glycosylation (CDG) syndromes.[6,7] Their diagnosis is based on the identification of underglycosylated transferrin, either by isoelectric focusing or mass-spectrometry analyses. Clinically, CDG syndromes are characterized by psychomotor retardation, ataxia, failure to thrive, dysmorphic features, and coagulopathies. To date, 18 different CDG subtypes have been described: 12 types in group I CDG and six in group II. Group I CDG results in the disrupted synthesis of the oligosaccharide chain, whereas group II CDG is defined as defects in the processing of the protein-bound glycan.[6] In eukaryotic cells, the key step of the N-glycosylation is mediated by the oligosaccharyltransferase (OTase), an oligomeric membrane-protein complex that catalyzes the transfer of preassembled high-mannose oligosaccharide onto asparagine residues of nascent polypeptides entering the lumen of the endoplasmic reticulum.[8] There are at least two mammalian OTase complexes that differ by the presence of N33/TUSC3 (MIM 601385) or IAP. These complexes are composed of seven proteins: Ribophorin I (MIM 180470), Ribophorin II (MIM 180490), OST48 (MIM 602202), DAD1 (MIM 600243), STT3 A/B (MIM 601134, MIM 608605), OST4 (MIM 604059), and N33/TUSC3 or IAP,[8] and, to date, no mutation in any of these subunits has ever been highlighted in a human disease.

In this article, we show that mutations in two OTase-subunit genes, *N33/TUSC3* and *IAP* (also named *MAGT1*), the *Ost3* and *Ost6 Saccharomyces cerevisae* human orthologs, respectively, result in NSMR. These data expand the spectrum of the CDG syndromes and emphasize the crucial role of glycosylation activity in higher brain functions and cognitive development.

[1]Laboratoire de Génétique et Epigénétique des Maladies Métaboliques, Neurosensorielles et du Développement (INSERM U781), Université Paris Descartes, Hôpital Necker-Enfants Malades, F-75015 Paris, France; [2]Laboratory for Molecular Diagnostics, Center for Human Genetics, University of Leuven, 3000 B-Leuven, Belgium; [3]Unité Mixte de Recherche CNRS/USTL 8576, Glycobiologie Structurale et Fonctionnelle, IFR 147, Université des Sciences et Technologies de Lille 1, F-59655 Villeneuve d'Ascq, France; [4]Cancer Genome Project, Wellcome Trust Sanger Institute, Wellcome Trust Genome Campus, Hinxton, CB10 1SA Cambridge, UK; [5]The Gold Service, Hunter Genetics and University of Newcastle, New South Wales, NSW 2308, Australia; [6]Department of Genetic Medicine, Women's and Children's Hospital, North Adelaide, SA 5005, Australia; [7]Department of Pediatrics and School of Molecular & Biomedical Science, University of Adelaide, Adelaide, SA 5005, Australia
*Correspondence: colleaux@necker.fr
DOI 10.1016/j.ajhg.2008.03.021.

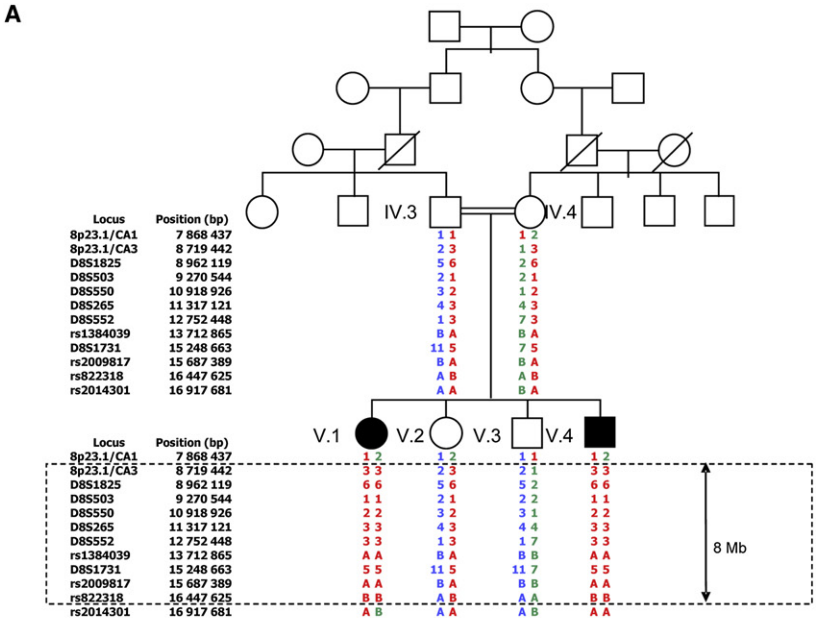

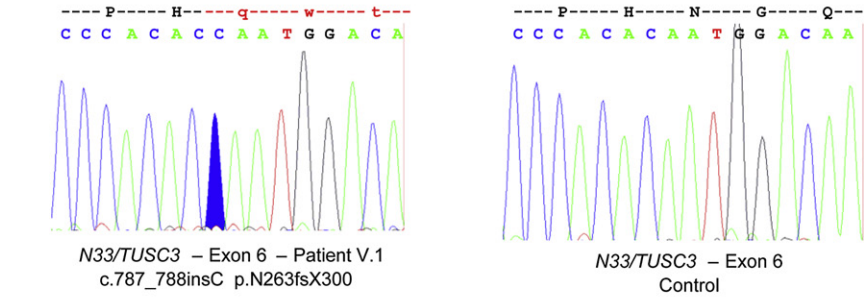

C

N33/TUSC3 mutation	QMWNHIRGPPYAHKNPH***qwtselhsweqpgsvcgrithy***
H.sapiens N33-1	QMWNHIRGPPYAHKNPHNGQVSYIHGSSQAQFVAESHII
H.sapiens N33-2	QMWNHIRGPPYAHKNPHNGQVSYIHGSSQAQFVAESHII
M.musculus	QMWNHIRGPPYAHKNPHNGQVSYIHGSSQAQFVAESHII
R.norvegicus	QMWNHIRGPPYAHKNPHNGQVSYIHGSSQAQFVAESHII
C.elegans	QMWNHIRGPPFMITNPNTKEPSFIHGSTQFQLIAETYIV
S.cerevisiae	YMFNQIRNTQLAGVGPKGEVMYFLPNEFQHQFAIETQVM

Figure 1. Genetic Analysis of Family 1
(A) Pedigree of family 1. The black symbols indicate the affected individuals. Autozygosity mapping was performed with Affymetrix GeneChip Human Mapping 10K for individuals IV.3, IV.4, and V.1 to V.4. Haplotypes are shown beneath each genotyped individual. Markers are from telomere to centromere, and their positions, based on the UCSC Genome browser, are indicated in bp.
(B) Electropherograms of *N33/TUSC3* exon 6 in an affected patient (left) and a control (right). DNA sequencing identified a one base-pair homozygous insertion c.787_788insC.
(C) N33/TUSC3 mutation and phylogenetic analysis of N33/TUSC3 proteins in various species. Amino acids are in italics; bold and underlined indicate the frame shift caused by *N33/TUSC3* mutation.

Material and Methods

Subjects and Families

Family 1

Affected children are 32 and 25 yr old, respectively. In both cases, pregnancy and delivery were uneventful (patient V.1: length 47 cm, weight 3050 g, head circumference 35.5 cm; patient V.4: length 49 cm, weight 3400 g, head circumference 35 cm), and no postnatal infection, toxic exposure, or significant head trauma was noted. Standard assessment revealed significant developmental delay in the two sibs (independent walking at 3 and 2.5 yr, respectively; no speech at 3 and 4 yr, respectively). Mental retardation could be estimated as severe and appeared nonprogressive.

Physical examination of both patients at 31 and 24 yr of age was unremarkable, with normal height, weight, and head circumference. Examination showed no malformations and normal metabolic screening (amino acid chromatography, blood lactate and pyruvate levels, liver function, and ammonemia). Molecular testing ruled out fragile X syndrome. High-resolution chromosome analysis, bone X-rays, cerebral MRI, and electroencephalogram were all normal.

Family 2

In this sibship of five children (one healthy girl, two girls with mild MR, and two boys with severe MR), only one affected boy (III.5, 62 yr old) is still alive; the other affected individuals (III.6) are deceased of liver or cervical cancer. The two affected males had a similar phenotype with the same degree of handicap. Both were in educational classes for the moderately handicapped. They were both able to hold a limited conversation; neither learned to read or write. Both were on disability pensions as adults. III.5 is in protected employment in a gardening team, and he lives independently and cooks his own meals but is visited very regularly by his sister, who supervises his affairs. When 59 yr old, he had normal growth parameters (height 166 cm; head circumference 57 cm). Their mother (II.2) was described as slow. One sister (III.4) who is deceased was in a special class for the mildly handicapped at school but was not as slow as the brothers.

Microarray Analysis

The 10K Array contains 11,555 single-nucleotide polymorphisms (SNPs) covering the whole human genome with a mean genetic map distance of 0.32 cM. The average distance between the SNPs is 210 kb, and the average heterozygosity of these SNPs is

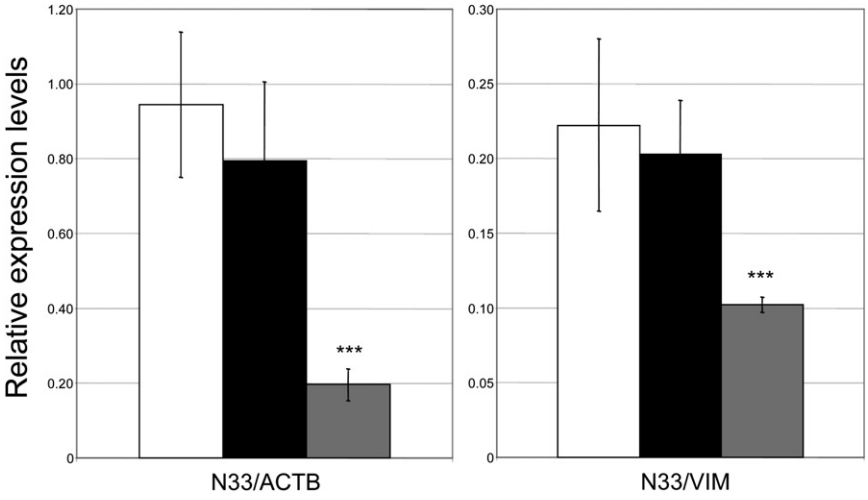

Figure 2. Quantitative PCR Analysis of *N33/TUSC3* mRNA

N33/TUSC3 expression in fibroblasts from two controls (black and white bars) and patient V.1 (gray bar). Data are normalized to *Beta-actin* (*ACTB*) or *Vimentin* (*Vim*). Means are given ± standard deviation (n = 4 to 8 independent RT-PCR). ***, $p < 0.001$ as compared to controls, Student's t test.

0.37. According to the manufacturer's instructions, 250 ng total genomic DNA was digested with a restriction enzyme (XbaI) and ligated to adaptors that recognize the cohesive 4 bp overhangs. Amplification, purification, labeling, and hybridization of PCR products were performed as recommended by the manufacturer. Results were analyzed with the GeneChip DNA Analysis software 3.0 (GDAS 3.0), and parametric linkage analyses were subsequently done with the Merlin program.

Mutation Screening of the *N33/TUSC3* and *IAP* Genes

Blood samples were obtained from siblings and their parents of family 1 after informed consent, and genomic DNA was isolated from blood leucocytes with the Nucleon kit (Amersham) according to the manufacturer's instructions. Genomic DNA from family 2 probands was isolated, after informed consent, from a lymphoblastoid cell line (patient III.5), from a Guthrie test sample (patient III.6), and from blood samples (patient III.2, III.3, IV.1, IV.2, and IV.3). Specific primers for PCR amplification of exons and splicing junctions of *N33/TUSC3* and *IAP* were designed on the basis of their sequence data from the GenBank database (NT_030737 and NT_113965, primer sequences are available on request). PCR products were purified with Exo-SAP (Amersham) and directly sequenced on an automated sequencer (ABI 3130xl, Applied Biosystems) via the dye-terminator method.

Expression Analyses of the *N33/TUSC3* and *IAP* Genes by RT-PCR

Selected RNAs from the Total Human RNA Master Panel II (Clontech) were subjected to reverse transcription with the SuperScript First-Strand Synthesis System (Invitrogen). Specific primers for PCR amplification of *N33/TUSC3*, *IAP*, and *Vimentin* (*Vim*) mRNA were designed on the basis of their sequence data from the GenBank database (NM_178234, NM_032121, and BC000163 respectively,): *N33/TUSC3*, forward 5′-GTTCTGTGTGCAGGCAAGCTA-3′ and reverse 5′-GGATAGCCGTGGTACTTGG-3′; *IAP*, forward 5′-CGTCATGTTCACTGCTCTCC-3′ and reverse 5′-CGAAGATACACAAGTCCACC-3′; and *Vim*, forward 5′-ACCAGCTAACCAACGACAAA-3′ and reverse 5′-TGCTGTTCCTGAATCTGAGC-3′.

Quantitative Real-Time RT-PCR

The level of *N33/TUSC3*, *Vimentin* (*Vim*), and *Beta-actin* (*ACTB*) mRNA expression were studied with specific primers designed according to GenBank sequence database: *N33/TUSC3*, forward 5′-GAACGGATGTTCATATTCGGGT-3′ and reverse 3′-CGCTTAAAGCAAACCTCCAACAA-5′; *Vim*, forward 5′-ACCAGCTAACCAACGACAAA-3′ and reverse 5′-TGCTGTTCCTGAATCTGAGC-3′; and *ACTB*, forward 5′-AGATCAAGATCATTGCTCCTCC-3′ and reverse 5′-AAAACAAATAAAGCCATGCCAATCT-3′. The quantitative assays were set up with the Light Cycler system with FastStart DNA Master^{PLUS} SYBR Green I (Roche). PCRs were performed with 5 μl of diluted cDNA template, forward and reverse primers (5 pmol each), and SYBR Green Master^{PLUS} Mix (4 μl) at a final volume of 20 μl. Each reaction was performed at an annealing temperature of 60°C and for 40 cycles. Melting-curve analysis was performed to assess the specificity of each transcript amplified. All reactions were performed in duplicate. For each amplification, a standard calibration using a control cDNA with different dilutions was performed. Relative expression was assessed with the calculated concentration in respect to the standard, so that a ratio of 1 represents an average ratio between *N33/TUSC3* mRNA and *Vim* or *ACTB* mRNA in control samples.

Cell Culture

Primary fibroblasts from patients and controls were cultured at 37°C under 5% CO2 in RPMI 1640/Glutamax (Invitrogen) supplemented with 10% of fetal calf serum (Invitrogen).

Release of the N-Linked Oligosaccharides and Clean-Up Procedure of the PNGase F-Released N-Glycans

Twenty microliters of serum were dried in a vacuum centrifuge. The N-glycans were released and purified as previously described.[9]

Permethylation of the Glycans and MALDI-TOF-MS

Permethylation of the freeze-dried glycans and MALDI-TOF-MS analyses of permethylated glycans were performed as described elsewhere.[9]

Metabolic Labeling with [2-^{3}H]mannose and [^{35}S]methionine

Fibroblasts (5×10^5 cells/well) were grown in DMEM supplemented with 10% of fetal calf serum. The next day, cells were metabolically labeled for 20, 40, and 60 min, respectively, in MEM free of methionine and cysteine, supplemented with 16 μCi/ml [2-^{3}H]mannose and 5 μCi/ml [^{35}S]methionine per well. Cells were then washed twice with ice-cold phosphate-buffered saline (PBS; pH 7.4) and scrapped into 1 ml of $CHCl_3$/MeOH/H_20 (1/2/2 v/v). The proteins were extracted and resuspended in 1% SDS. Radioactivity incorporated was determined by liquid scintillation counting.

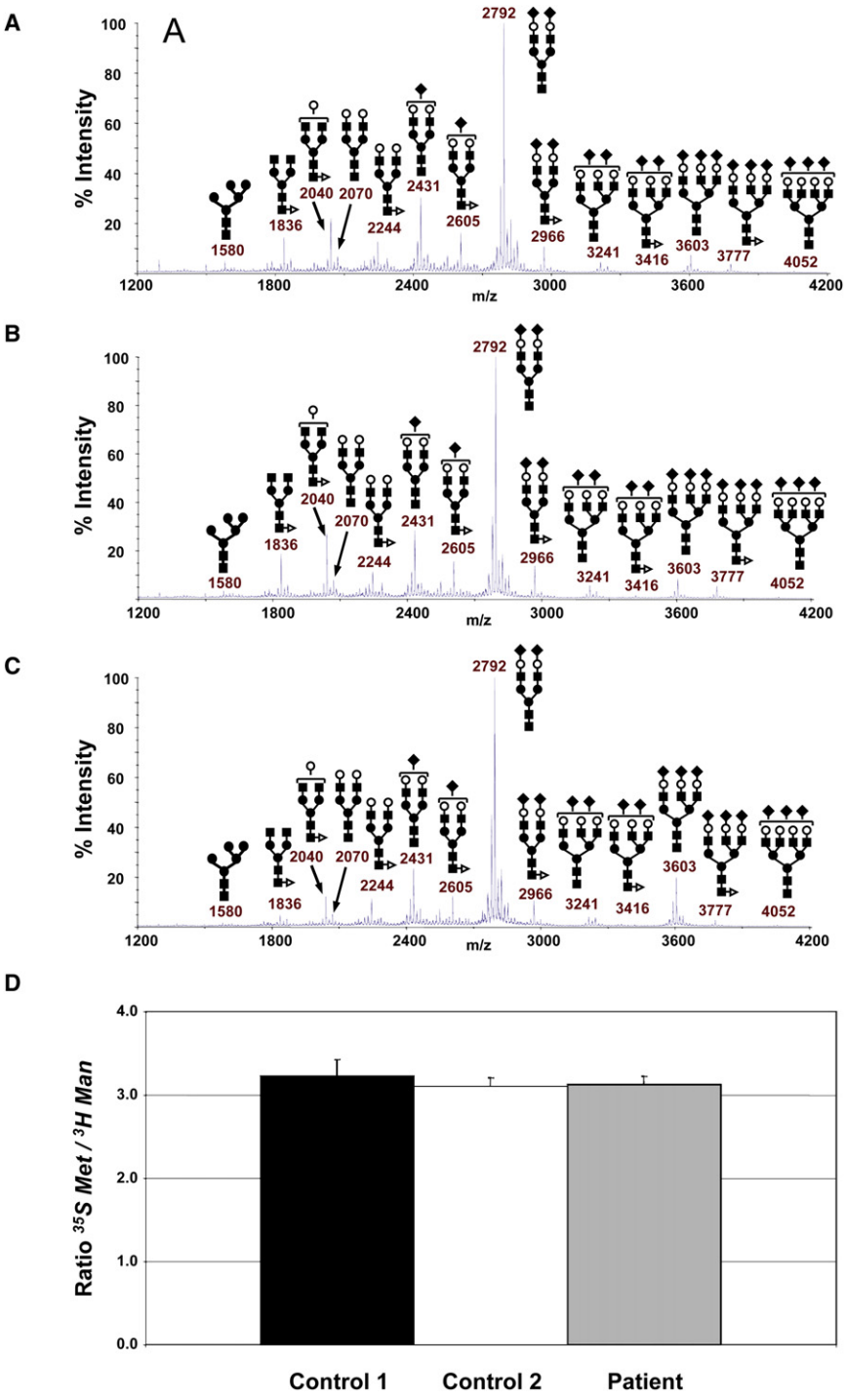

Figure 3. MALDI-TOF MS Analysis of Total Human Serum N-Glycome

(A) Spectrum obtained from of a normal individual.

(B and C) Spectra obtained from the two affected children of family 1, V.4 and V.1, respectively. Only the structures of the major N-glycans are given. A minor portion of the monofucosylated glycans carries fucose on an antenna rather than the core. Galactose (open circles), mannose (closed circles), GlcNAc (closed squares), fucose (open triangles), and NeuAc (closed diamonds) are shown.

(D) Incorporation of [2-^{3}H]mannose and [^{35}S]methionine was determined after metabolic labeling of fibroblasts for 20, 40, and 60 min. Shown is the average ratio of [^{35}S]methionine versus [2-^{3}H]mannose incorporation into proteins of two independent experiments.

Results

Linkage Analysis of Family 1

We had the opportunity to study two sibs born to second-cousin French parents (family 1, Figure 1A) and presenting NSMR. Autozygosity mapping, with the Affymetrix GeneChip Human Mapping 10K array, in both affected and healthy children and in parents identified a unique homozygous region on chromosome 8p22-p23.1 (Figure 1A). Further polymorphic marker analyses reduced the critical region to an 8 Mb interval (maximum LOD score Zmax = 2.65 at $\theta = 0$ for marker D8S552) encompassing 25 known genes and a dozen predicted genes. On the basis of their expression in the brain and their putative role in the central nervous system (CNS), four genes were sequenced (*TNKS* [MIM 603303], *FDFT1* [MIM 184420], *NEIL2* [MIM 608933], and *SOX7*), and then *N33/TUSC3* (*Ost3 Saccharomyces cerevisae* ortholog) was. The *N33/TUSC3* transcription unit encompasses 11 exons and encodes two isoforms (1 and 2) sharing the first nine exons but containing a distinct 3′ exon. This alternative splicing results in the synthesis of two proteins differing by their five C-terminal amino acids.

Direct sequencing of all coding exons and exon-intron junctions identified a 1 bp homozygous insertion in exon 6, c.787_788insC (Figure 1B). This frameshift mutation (p.N263fsX300) cosegregated with the disease and was predicted to cause the premature termination of translation and the synthesis of a truncated N33/TUSC3 protein lacking the 84 C-terminal amino acids (Figure 1C). This variant was not found in 250 control chromosomes from various ethnic origins (90% of European descent, 10% North African).

Functional Analysis of *N33* Mutation

The consequence of the c.787_788insC sequence variant on *N33/TUSC3* expression was assessed by reverse-transcription

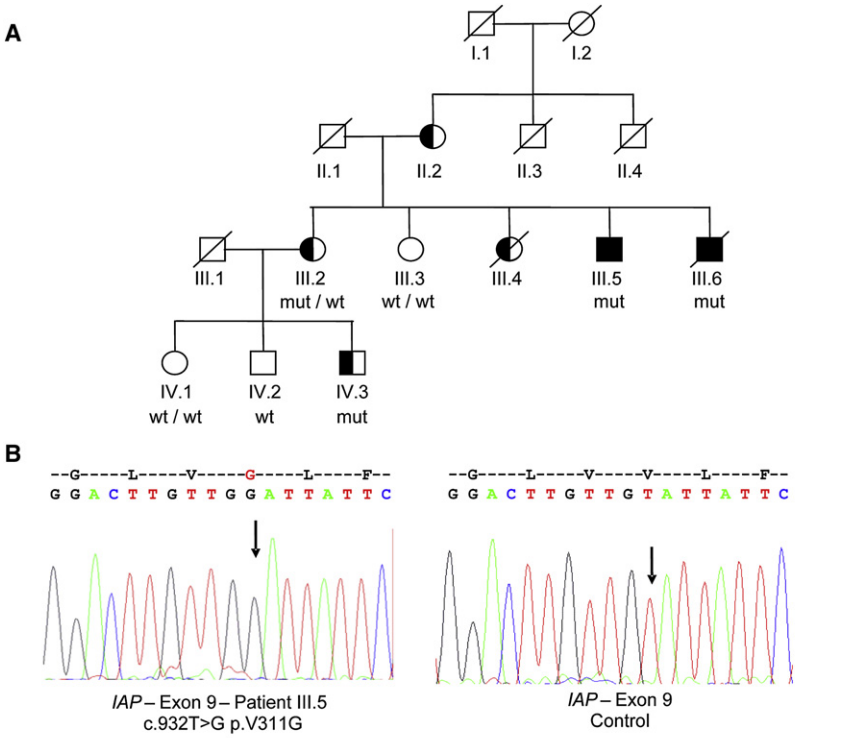

Figure 4. Genetic Analysis of Family 2
(A) Pedigree of family 2. The black symbols indicate individuals presenting severe MR, the white and black symbols indicate individuals presenting mild MR, and the white symbols indicate the nonaffected individuals. Carriers of mutated (mut) or wild-type (wt) alleles are indicated.
(B) Electropherograms of *IAP* exon 9 in one affected boy of family 2 (left) and a control (right). DNA sequencing identified a missense mutation c.932T→G.
(C) IAP mutation and phylogenetic analysis of IAP proteins in various species. The arrow and bold amino acids indicate the substitution caused by the mutation.

PCR (RT-PCR) of cultured skin fibroblast RNAs of patient V.1. No aberrant mRNA but a reduced amount of transcript was observed. Quantitative real-time RT-PCR (qRT-PCR) with the Light Cycler technology showed a significantly reduced amount of *N33/TUSC3* mRNA in patient V.1 fibroblasts as compared to two controls for which two housekeeping genes were used (from 54.1% to 79.1% of reduction, $p < 0.001$, Figure 2). These results suggest that the primary effect of this frameshift mutation is nonsense-mediated decay of the *N33/TUSC3* mRNA.

Glycosylation Analysis in Cells Harboring the *N33* Mutation

Because isoelectric focusing showed no alteration of serum-transferrin glycosylation (data not shown), we undertook the mass-spectrometry characterization of N-glycan structures of glycoproteins isolated from the patient's serum.[10] The MALDI-TOF spectra of permethylated N-glycans obtained by deglycosylation of serum glycoproteins of patients V.1 and V.4 were compared to a control serum sample (Figures 3A–3C). A total of 26 oligosaccharide structures were individualized, but neither qualitative nor quantitative differences were observed. This result suggests that the *N33/TUSC3* mutation had no overt effect on the glycosylation pattern of serum proteins but probably affected specific cell types. To further investigate whether N33/TUSC3 subunit mutation could alter glycan transfer, we compared the incorporation of [2-^{3}H]mannose into nascent proteins in control and patient cells. After metabolic labeling, the ratio of [^{35}S]methionine/[2-^{3}H]mannose was similar in patient and control fibroblasts (Figure 3D), suggesting that the *N33/TUSC3* mutation did not lead to global N-glycan transfer impairment.

Mutation Screening of *N33* Paralog, the *IAP* Gene

The OTase subunit Ost3p and its paralog Ost6p have been originally identified in yeast.[11,12] They share 20% of sequence identity and display a strikingly similar membrane topology. In addition to the *N33/TUSC3* gene, mammalian genomes also contain an *Ost6* ortholog, named *IAP*, which maps to Xq21.1 and composed of ten coding exons. We therefore investigated whether *IAP* gene mutations could account for MR. We first sequenced all coding exons and exon-intron junctions in a series of 18 probands in XLMR families linked to the Xq21.1 region, and no mutation was found. Then, we took advantage of the International Genetics of Learning Disabilities program, which

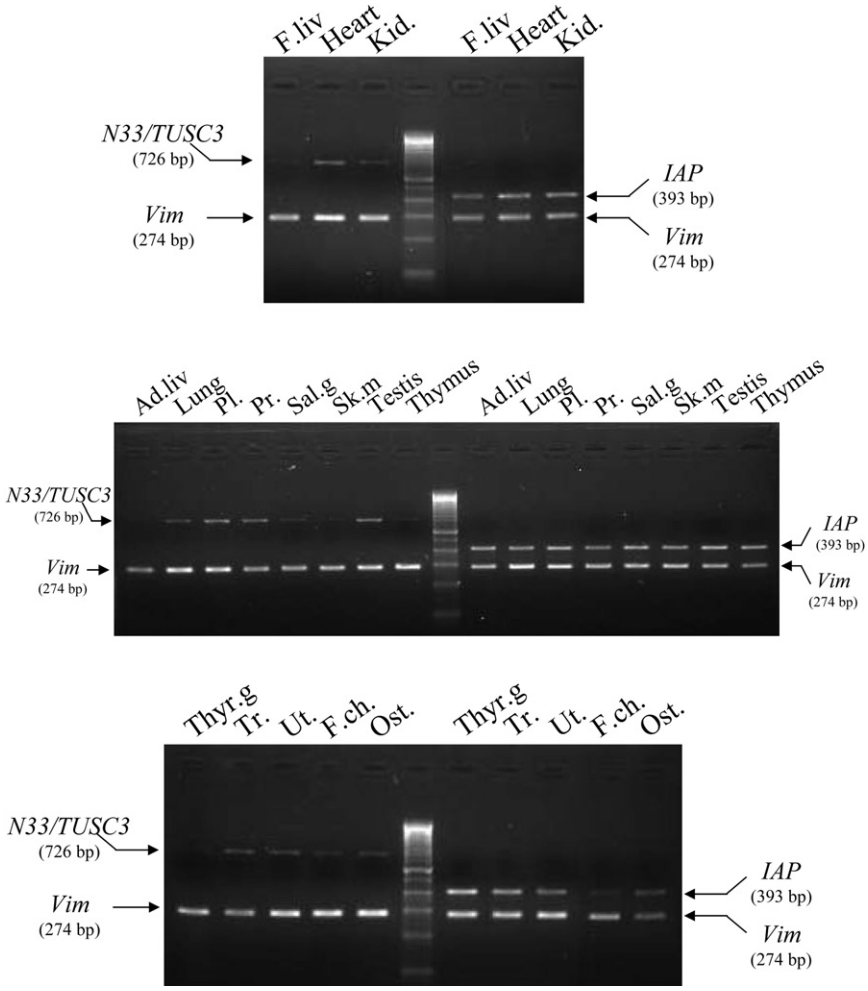

Figure 5. Expression Analyses of *N33/TUSC3*, *IAP*, and *Vimentin*

Expression was asseyed by RT-PCR on adult and fetal total RNA isolated from various tissues (Clontech): fetal liver (F.liv), heart, kidney (Kid.), adult liver (Ad.liv), lung, placenta (Pl.), prostate (Pr.), salivary gland (Sal.g), skeletal muscle (Sk.m), testis, thymus, thyroid gland (Thyr.g), trachea (Tr.), uterus (Ut.), fetal chondrocytes (F.ch), and osteoblasts (Ost.). Amplicon length of *N33/TUSC3*, *IAP*, and *Vimentin* (*Vim*) are indicated in bp.

undertook a systematic, high-throughput mutational screen of the VEGA-annotated X chromosome gene set (737 genes) in 250 MR families.[13] One proband per family had been previously tested for karyotype anomalies, *FMR1* mutations, and mutations in the 61 known XLMR genes. Samples were then subsequently screened for variants in coding exons and splice junctions of the remaining 737 VEGA-annotated X chromosome genes (Vega Genome Browser) by bidirectional, PCR-based direct sequencing. A single variant in the *IAP* gene was identified in the proband of an Australian family (c.932T→G, p.V311G; family 2, Figure 4B). The p.V311G variant cosegregated with the disease (Figure 4A) and involved a highly conserved amino acid (Figure 4C). This variant was not found in 267 control X chromosomes. Neither *N33/TUSC3* nor *IAP* mRNA was expressed in lymphoblastoid cell lines, and no skin fibroblasts from this patient were available, ruling out the possibility of testing the impact of this mutation at the RNA level.

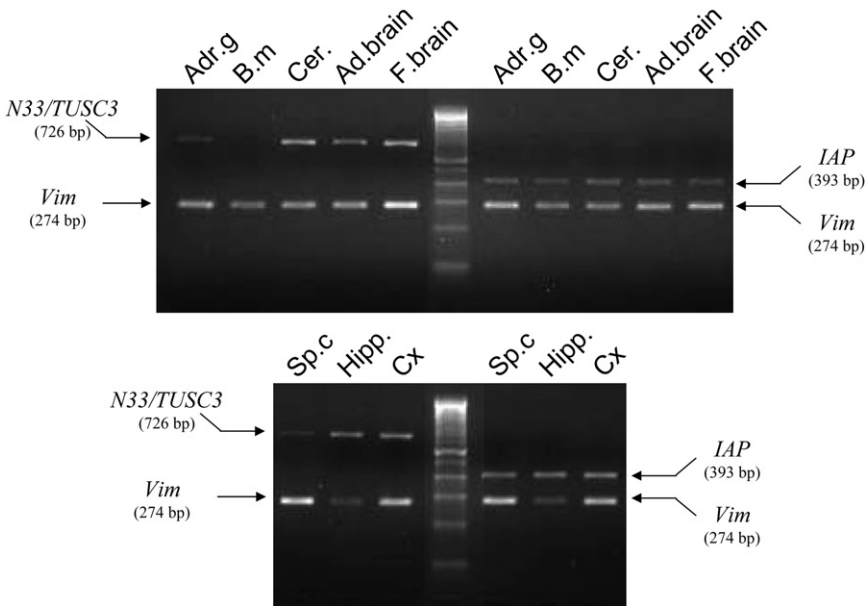

Figure 6. Expression Analyses of *N33/TUSC3*, *IAP*, and *Vimentin* (*Vim*) mRNAs in Adult and Fetal Brain Structures

Expression was tested by RT-PCR on adult and fetal structures (Clontech): adrenal gland (Adr.g), bone marrow (B.m), cerebellum (Cer.), adult brain (Ad.brain), fetal brain (F.brain), spinal cord (Sp.c), hippocampus (Hipp.), and cortex (Cx). Amplicon length of *N33/TUSC3*, *IAP*, and *Vimentin* (*Vim*) are indicated in bp.

Tissue Distribution of *N33* and *IAP* mRNA

To get further insight in the functional consequences of the *N33/TUSC3* and *IAP* mutations, we undertook the analysis of their expression by RT-PCR in various adult and fetal tissues. As shown in Figure 5, both genes were found ubiquitously expressed, including in fetal and adult brain structures tested (Figure 6A). Noticeably, *N33/TUSC3* expression was found more abundant in total fetal brain (Figure 6A).

Discussion

Surprisingly, although the OTase complex plays a key role in N-glycosylation, no OTase subunit mutations have been hitherto identified in human. To our knowledge, our data provide the first demonstration that mutations in OTase subunits are responsible for isolated cognitive deficit, thus expanding the spectrum of CDG syndromes. Interestingly, a separate study has identified a homozygous deletion of a portion of the *N33/TUSC3* gene that segregates with MR in a large consanguineous family, further supporting the conclusion that N33/TUSC3 defects are responsible for autosomal-recessive nonsyndromic MR.[14]

In the meantime, these results raise the issue of understanding how mutations in genes involved in an essential and ubiquitous cellular process could result in a CNS-restricted phenotype.

It is worth remembering that in *Saccharomyces cerevisae*, two distinct isoforms of OTase exist, only differing by the inclusion of either Ost3p or Ost6p.[15,16] Neither Ost3p nor Ost6p is absolutely required for OTase activity. Indeed, disruption of either yeast *Ost3* or *Ost6* genes only caused a moderate hypoglycosylation phenotype, whereas the double *Δost3Δost6* mutation led to a severe N-glycosylation defect.[12] Moreover, when overexpressed, they could displace each other, suggesting a dynamic regulation of the complex.[12] Our data suggest that it might also be the case in human, at least in fibroblasts cells, where IAP could functionally compensate for the lack of N33/TUSC3 protein, thus resulting in a normal N-glycosylation in all but neuronal cells.

Alternatively, the two proteins could also be involved in the glycosylation of a subset of proteins essential for normal brain function. This hypothesis is further supported by the data from B. Schultz and colleagues, who demonstrated that Ost3p and Ost6p subunits may determine, to some extent, the substrate specificity of OTase complexes (personal communication). Indeed, on the basis of a multidisciplinary approach, this group has demonstrated that in yeast, Ost3p and Ost6p have disulfide reductase and peptide-binding activities, which modulate the oxidative folding of specific glycoproteins, thereby allowing glycosylation of defined acceptor sites. In addition, their results demonstrate that each protein has distinct site specificity, because different sites were underglycosylated in *Ost3* or *Ost6* yeast mutants. Given that most N-glycosylation sites do not require reductase activity, these data are consistent with the absence of a hypoglycosylation phenotype of standard glycoproteins observed in patients and point to a specific hypoglycosylation of proteins that are required for normal higher-brain functions.

Cognitive dysfunction is generally regarded as the consequence of a defect in synapse formation and plasticity, especially in the postnatal stage, during learning and acquisition of intellectual performance and emotional behavior. Some evidence supports a close link between long-term potentiation (LTP) and memory storage.[17,18] Along these lines, it is worth remembering that disruption of N-glycosylation by specific inhibitors, such as Tunicamycin or Swainsonine, had a direct effect on transition of short-term potentiation into a long-lasting maintenance of hippocampal LTP.[19] Further studies will hopefully clarify the nature of the specific carbohydrate structure and the identity of the proteins carrying such plasticity-relevant structures. Yet, the involvement of L1 and neural cell-adhesion molecules (L1CAM and NCAM) is already supported by several observations, and polysialic acid (PSA) modification of NCAM supports the critical role of glycosylation in synaptic plasticity and memory consolidation.[20–23] Furthermore, in brain, PSA is attached to NCAM in a developmentally regulated manner. PSA-NCAM is associated with morphogenetic changes during development (cell migration, synaptogenesis), whereas PSA-NCAM is low in adult brain except in regions with a high degree of plasticity (hippocampus, hypothalamus, olfactory bulb).[24,25] PSA has a high negative-charge density, which might decrease adhesion strength of cell interactions[26] and be needed for synapse remodeling. Facilitating synaptic plasticity induces formation and stabilization of a long-lasting memory trace. Finally, mutations in *L1CAM* are associated with neurodevelopmental disorders including X-linked hydrocephalus and MR, and several amino acid substitutions identified in patients have been shown to alter the glycosylation pattern of this protein.[27]

In conclusion, the results reported here emphasize the crucial role of OTase activity in higher-brain function and expand the field of the pathophysiology of mental retardation.

Acknowledgments

We are thankful to J. Chelly for providing us with samples of 18 boys with XLMR, to J.P. Jais for LOD score calculation, and to the patients and families for their cooperation. We also want to thank M. Aebi for sharing unpublished data regarding the functional analyses of yeast *Ost3* and *Ost6* genes and for helpful discussion. This study was supported in part by the Centre National de la Recherche Scientifique (CNRS), the Agence Nationale de la Recherche (ANR), the Ministère de la Recherche et de l'Enseignement Supérieur (France), the Fund for Scientific Research (Flanders, Belgium), and Mizutani Foundation for Glycoscience (Japan). The Mass Spectrometry facility used in this study was funded by the European Community (FEDER), the Région Nord-Pas de Calais (France), and the Université des Sciences et Technologies de Lille I.

Received: December 20, 2007
Revised: March 12, 2008
Accepted: March 16, 2008
Published online: May 1, 2008

Web Resources

The URLs for data presented herein are as follows:

Ensembl, http://www.ensembl.org/
Fondation Jean Dausset-CEPH (Centre d'Etude du Polymorphisme Humain), http://www.cephb.fr/cephdb/php/eng/index.php/
GenBank, http://www.ncbi.nlm.nih.gov/Genbank/
Genecards, http://www.genecards.org/
The International Genetics of Learning Disabilities program (IGOLD), http://goldstudy.cimr.cam.ac.uk/
Online Mendelian Inheritance in Man (OMIM), http://www.ncbi.nlm.nih.gov/OMIM/

References

1. American Psychiatric Association (1995). Diagnostic and Statistical Manual of Mental Disorders, 4th revised edition, DSM-IV-R (Washington, D.C.: APA).
2. Molinari, F., Rio, M., Meskenaite, V., Encha-Razavi, F., Auge, J., Bacq, D., Briault, S., Vekemans, M., Munnich, A., Attie-Bitach, T., et al. (2002). Truncating neurotrypsin mutation in autosomal recessive nonsyndromic mental retardation. Science *298*, 1779–1781.
3. Higgins, J.J., Pucilowska, J., Lombardi, R.Q., and Rooney, J.P. (2004). A mutation in a novel ATP-dependent Lon protease gene in a kindred with mild mental retardation. Neurology *63*, 1927–1931.
4. Basel-Vanagaite, L., Attia, R., Yahav, M., Ferland, R.J., Anteki, L., Walsh, C.A., Olender, T., Straussberg, R., Magal, N., Taub, E., et al. (2006). The CC2D1A, a member of a new gene family with C2 domains, is involved in autosomal recessive nonsyndromic mental retardation. J. Med. Genet. *43*, 203–210.
5. Motazacker, M.M., Rost, B.R., Hucho, T., Garshasbi, M., Kahrizi, K., Ullmann, R., Abedini, S.S., Nieh, S.E., Amini, S.H., Goswami, C., et al. (2007). A defect in the ionotropic glutamate receptor 6 gene (GRIK2) is associated with autosomal recessive mental retardation. Am. J. Hum. Genet. *81*, 792–798.
6. Eklund, E.A., and Freeze, H.H. (2006). The congenital disorders of glycosylation: A multifaceted group of syndromes. NeuroRx *3*, 254–263.
7. Freeze, H.H. (2006). Genetic defects in the human glycome. Nat. Rev. Genet. *7*, 537–551.
8. Kelleher, D.J., and Gilmore, R. (2006). An evolving view of the eukaryotic oligosaccharyltransferase. Glycobiology *16*, 47R–62R.
9. Faid, V., Chirat, F., Seta, N., Foulquier, F., and Morelle, W. (2007). A rapid mass spectrometric strategy for the characterization of N- and O-glycan chains in the diagnosis of defects in glycan biosynthesis. Proteomics *7*, 1800–1813.
10. Morelle, W., and Michalski, J.C. (2007). Analysis of protein glycosylation by mass spectrometry. Nat. Protoc. *2*, 1585–1602.
11. Knauer, R., and Lehle, L. (1999). The oligosaccharyltransferase complex from Saccharomyces cerevisiae. Isolation of the OST6 gene, its synthetic interaction with OST3, and analysis of the native complex. J. Biol. Chem. *274*, 17249–17256.
12. Schwarz, M., Knauer, R., and Lehle, L. (2005). Yeast oligosaccharyltransferase consists of two functionally distinct subcomplexes, specified by either the Ost3p or Ost6p subunit. FEBS Lett. *579*, 6564–6568.
13. Tarpey, P.S., Stevens, C., Teague, J., Edkins, S., O'Meara, S., Avis, T., Barthorpe, S., Buck, G., Butler, A., Cole, J., et al. (2006). Mutations in the gene encoding the Sigma 2 subunit of the adaptor protein 1 complex, AP1S2, cause X-linked mental retardation. Am. J. Hum. Genet. *79*, 1119–1124.
14. Garshasbi, M., Hadavi, V., Habibi, H., Kahrizi, K., Kariminejad, R., Behjati, F., Tzschach, A., Najmabadi, H., Ropers, H.H., and Kuss, A.W. (2008). A defect in the *TUSC3* gene is associated with autosomal-recessive mental retardation. Am. J. Hum. Genet. *82*, this issue, 1158–1164.
15. Spirig, U., Bodmer, D., Wacker, M., Burda, P., and Aebi, M. (2005). The 3.4-kDa Ost4 protein is required for the assembly of two distinct oligosaccharyltransferase complexes in yeast. Glycobiology *15*, 1396–1406.
16. Yan, A., and Lennarz, W.J. (2005). Two oligosaccharyl transferase complexes exist in yeast and associate with two different translocons. Glycobiology *15*, 1407–1415.
17. Bliss, T.V., and Collingridge, G.L. (1993). A synaptic model of memory: Long-term potentiation in the hippocampus. Nature *361*, 31–39.
18. Fedulov, V., Rex, C.S., Simmons, D.A., Palmer, L., Gall, C.M., and Lynch, G. (2007). Evidence that long-term potentiation occurs within individual hippocampal synapses during learning. J. Neurosci. *27*, 8031–8039.
19. Matthies, H. Jr., Kretlow, J., Matthies, H., Smalla, K.H., Staak, S., and Krug, M. (1999). Glycosylation of proteins during a critical time window is necessary for the maintenance of long-term potentiation in the hippocampal CA1 region. Neuroscience *91*, 175–183.
20. Muller, D., Wang, C., Skibo, G., Toni, N., Cremer, H., Calaora, V., Rougon, G., and Kiss, J.Z. (1996). PSA-NCAM is required for activity-induced synaptic plasticity. Neuron *17*, 413–422.
21. Bonfanti, L. (2006). PSA-NCAM in mammalian structural plasticity and neurogenesis. Prog. Neurobiol. *80*, 129–164.
22. Lopez-Fernandez, M.A., Montaron, M.F., Varea, E., Rougon, G., Venero, C., Abrous, D.N., and Sandi, C. (2007). Upregulation of polysialylated neural cell adhesion molecule in the dorsal hippocampus after contextual fear conditioning is involved in long-term memory formation. J. Neurosci. *27*, 4552–4561.
23. Senkov, O., Sun, M., Weinhold, B., Gerardy-Schahn, R., Schachner, M., and Dityatev, A. (2006). Polysialylated neural cell adhesion molecule is involved in induction of long-term potentiation and memory acquisition and consolidation in a fear-conditioning paradigm. J. Neurosci. *26*, 10888–10898.
24. Gascon, E., Vutskits, L., and Kiss, J.Z. (2007). Polysialic acid-neural cell adhesion molecule in brain plasticity: From synapses to integration of new neurons. Brain Res. Rev. *56*, 101–118.
25. Kiss, J.Z., and Rougon, G. (1997). Cell biology of polysialic acid. Curr. Opin. Neurobiol. *7*, 640–646.
26. Rutishauser, U. (1996). Polysialic acid and the regulation of cell interactions. Curr. Opin. Cell Biol. *8*, 679–684.
27. Weller, S., and Gartner, J. (2001). Genetic and clinical aspects of X-linked hydrocephalus (L1 disease): Mutations in the L1CAM gene. Hum. Mutat. *18*, 1–12.